Fluctuation and resonance analysis for $^{11}B+^{12}C$, $^{7}Li+^{16}O$, and $^{10}B+^{13}C$ induced reactions

J. F. Mateja and G. L. Gentry*
Physics Department, Tennessee Technological University, Cookeville, Tennessee 38505

N. R. Fletcher, L. C. Dennis, and A. D. Frawley
Physics Department, Florida State University, Tallahassee, Florida 32306
(Received 18 November 1987)

Some heavy-ion resonance studies have suggested that entrance channel binding energies and, to a lesser extent, moments of inertia are important factors in determining whether or not a given entrance channel will exhibit resonances. To further investigate this question, two channels which lead to the ^{23}Na compound nucleus, $^{10}B+^{13}C$ and $^{7}Li+^{16}O$, have been studied. When combined with the results from an earlier $^{11}B+^{12}C$ investigation, an extensive set of data is now available to study the entrance channel dependence of heavy-ion resonance formation in ^{23}Na.

I. INTRODUCTION

Over the past 25 years, the formation of resonances in heavy-ion reactions has received considerable experimental and theoretical attention.[1-6] Because most early studies were focused on finding resonances in individual heavy-ion systems, some very fundamental questions related to heavy-ion resonance formation were not addressed. Relatively little was known, for example, about how resonance formation in a particular compound nucleus depended upon entrance channel.

A model proposed by Thornton *et al.*[2] suggests that the binding energies of the entrance channel nuclei and, to a lesser extent, their moments of inertia at the grazing distance, are the most important factors in determining which systems will resonate. This model has been shown to be consistent with resonance formation for different entrance channels leading to the ^{26}Al, ^{29}Si, and ^{30}Si compound systems.[3]

In the present work we test the applicability of this model to resonance formation in ^{23}Na. The ^{23}Na compound nucleus has been chosen for study for three reasons. First, this compound nucleus can be formed by three accessible entrance channels: $^{11}B+^{12}C$, $^{10}B+^{13}C$, and $^{7}Li+^{16}O$. Second, extensive studies of the ^{4}He, ^{8}Be, and elastic exit channels for the $^{11}B+^{12}C$ entrance channel have revealed the existence of many strong resonance-like structures.[4,5] Finally, knowledge of the angular momentum available to the compound nucleus is essential if one hopes to determine whether or not different entrance channels can populate the same compound nucleus states. The grazing and critical angular momenta for these entrance channels have been determined in earlier studies of fusion cross sections.[7]

The effect of the exit channel has been minimized by studying the same exit channels for each entrance channel. Since the ^{4}He, ^{8}Be, and elastic exit channels were studied in the earlier $^{11}B+^{12}C$ experiment, these were the exit channels focused upon in the present investigation.

II. EXPERIMENTAL PROCEDURES

The $^{7}Li+^{16}O$ and $^{10}B+^{13}C$ measurements were made using ^{7}Li, ^{16}O, ^{10}B, and ^{13}C beams from the Florida State University (FSU) super-FN tandem Van de Graaff accelerator. The particular reactions used in the present experiment, along with a summary of the projectile energy ranges, targets, and detector angle settings, are presented in Tables I and II. In addition, Table II contains a list of the residual excited states studied in the present experiment. A summary of the $^{11}B+^{12}C$ results[4,5] are also presented in Tables I and II.

For both the $^{7}Li+^{16}O$ and $^{10}B+^{13}C$ elastic scattering experiments, ΔE-E telescopes were used to identify the scattered particles. In the $^{10}B+^{13}C$ work, back-angle center-of-mass cross sections for the $^{13}C(^{10}B,^{10}B)^{13}C$ reaction were obtained by detecting the recoil ^{13}C nuclei. For the $^{16}O(^{7}Li,^{7}Li)^{16}O$ study, the back-angle data were obtained by inverting the target and projectile, i.e., by bombarding ^{7}Li targets with an ^{16}O beam.

In the ^{4}He measurements, the large positive reaction Q values, from 7.8 to 14.2 MeV, allowed unambiguous ^{4}He identification from inclusive singles spectra.

The ^{8}Be measurements were made using the FSU ^{8}Be zero-degree detection system[8] and the ^{8}Be eight-detector array.[9] In the ^{8}Be experiments, thin aluminum foils were placed over the detectors to eliminate the elastic scattering events. Because of these foils, however, no back-angle data for the higher excited states in ^{15}N could be obtained as the breakup alpha particles resulting from these interactions were stopped in the foils. In the $^{7}Li(^{16}O,^{8}Be)^{15}N$ reaction, an ^{16}O contaminant on the LiCl targets obscured all but the ground state group in ^{15}N.

Absolute cross sections for those experiments employing ^{13}C targets were obtained by measuring the yield of ^{16}O elastic scattering at 20 MeV at angles from 14° to 20° in the laboratory. In this energy and angular range the cross section is well described by the Rutherford-scattering formula. For the $^{10}B(^{13}C,^{8}Be)^{15}N$ experiment, the ^{10}B target thickness was determined by elastically

TABLE I. Summary of reactions used in the present experiment.

Reaction	E_{lab} (MeV)	$E_{c.m.}$[a] (MeV)	$E_x(^{23}Na)$ (MeV)	θ_{lab} (deg)
$^{13}C(^{10}B,^{13}C)^{10}B$	17.16–31.32	9.70–17.70	34.41–42.41	13.8
$^{13}C(^{10}B,^{4}He)^{19}F$	17.16–31.32	9.79–17.70	34.41–42.41	14.3, 23.4 32.5, 41.6
$^{10}B(^{13}C,^{8}Be)^{15}N$	20.71–38.18	9.00–16.60	33.71–41.31	7.5, 12.5 17.5
$^{7}Li(^{16}O,^{7}Li)^{16}O$	20.00–50.23	6.09–15.29	25.79–34.99	14.6, 24.6 34.6, 44.6
$^{16}O(^{7}Li,^{4}He)^{19}F$	10.30–22.40	7.17–15.58	26.87–35.28	32.5, 45.0 57.5
$^{7}Li(^{16}O,^{8}Be)^{15}N$	20.00–51.20	6.09–15.58	25.79–35.28	0, 7.5, 12.5, 17.5, 22.5, 27.5, 32.5, 37.5
$^{12}C(^{11}B,^{11}B)^{12}C$[b]	18.80–34.10	9.81–17.79	28.01–35.99	14.6, 19.6, 24.6, 49.6, 59.6
$^{12}C(^{11}B,^{4}He)^{19}F$[b]	18.80–34.10	9.81–17.79	28.01–35.99	19.6, 29.6, 39.6
$^{12}C(^{11}B,^{8}Be)^{15}N$[b]	18.80–34.10	9.81–17.79	28.01–35.99	7.5, 12.5, 17.5, 22.5, 27.5, 32.5

[a]The center-of-mass energy step size was 0.1 MeV.
[b]Taken from Ref. 5.

scattering ^{16}O from the target at 15 MeV at angles of 25°–35°. Again the scattering was found to be due to the Coulomb force.

For those $^{7}Li+^{16}O$ experiments which employed an oxygen target, Rutherford scattering of 15 MeV ^{12}C from ^{16}O at angles of 20° and 22.5° was used to determine the oxygen thickness. Finally, the absolute cross sections for those excitation functions which used ^{7}Li targets were obtained by elastically scattering protons from the LiF and LiCl targets. The proton elastic scattering, performed at $E_{lab}=6.68$ MeV and $\theta_{lab}=95°$, was compared with the data of Bingham[10] to give absolute normalizations. In all of the above experiments, target nonuniformities, angle setting uncertainties, and statistical errors produced an uncertainty in the absolute cross sections of about 15%.

III. EXPERIMENTAL RESULTS AND ANALYSIS

The excitation functions for the $^{10}B+^{13}C$ and $^{7}Li+^{16}O$ entrance channels are presented in Figs. 1–6.

TABLE II. A summary of the reactions, targets, and excited states studied in the present experiment.

Reaction	Target	Residue excited state (MeV)
$^{13}C(^{10}B,^{13}C)^{10}B$	^{13}C	0.0
$^{13}C(^{10}B,^{4}He)^{19}F$	^{13}C	0.0–0.11–0.20, 1.35–1.46–1.55, 2.78, 3.91–4.00–4.03, 4.39–4.68, 5.34–5.63
$^{10}B(^{13}C,^{8}Be)^{15}N$	^{10}B	0.0, 5.27–5.30, 6.32, 7.15–7.30–7.56
$^{7}Li(^{16}O,^{7}Li)^{16}O$	LiF	0.0
$^{16}O(^{7}Li,^{4}He)^{19}F$	SiO_2	0.0–0.11–0.20, 1.35–1.46–1.55, 2.78, 3.91–4.00–4.03, 4.39–4.68
$^{7}Li(^{16}O,^{8}Be)^{15}N$	LiCl	0.0
$^{12}C(^{11}B,^{11}B)^{12}C$	^{12}C	0.0, 2.15(^{11}B), 4.43(^{12}C)–4.45(^{11}B)–5.02(^{11}B)
$^{12}C(^{11}B,^{4}He)^{19}F$	^{12}C	0.0–0.11–0.20, 1.35–1.46–1.56, 2.78
$^{12}C(^{11}B,^{8}Be)^{15}N$	^{12}C	0.0, 5.27–5.30, 6.32, 7.15–7.30–7.56

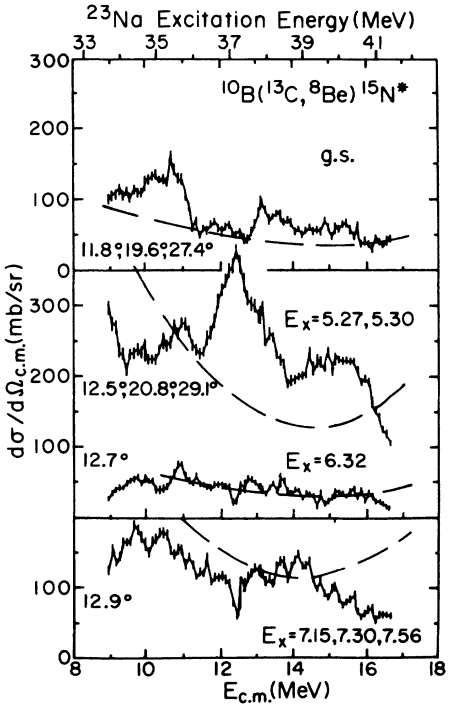

FIG. 1. Excitation functions for the $^{10}B+ {}^{13}C$ reaction leading to the ^{8}Be exit channel. The energies of the residual ^{15}N states are given in MeV. Center-of-mass angles, computed for the lowest energy of the excitation function, are those over which the excitation functions have been summed. The dashed curves represent the results of the Hauser-Feshbach analysis.

The excitation functions for the $^{11}B+ {}^{12}C$ case, taken from Ref. 5, are displayed in Figs. 7–9. Where possible, all of the results presented in these figures have been summed over angle in an effort to reduce the effect of statistical fluctuations.

A. Hauser-Feshbach analysis

Calculations of the compound nuclear cross sections for all of the reaction channels displayed in Figs. 1–9 have been made using the Hauser-Feshbach statistical model code Helga[11] (dashed lines). Details of the method of the calculations are identical to those presented in Ref. 12. The level density and optical model parameters used in the present calculations are presented in Tables III and IV, respectively. The critical angular momenta used in the Hauser-Feshbach analysis were extracted from the fusion cross sections of Ref. 7. The need for such a cutoff in angular momentum has been shown[13] to affect both the magnitude of the compound nuclear calculations and the relative cross sections for the different exit channels.

The ^{4}He and ^{8}Be absolute cross sections for the $^{11}B+ {}^{12}C$ and $^{10}B+ {}^{13}C$ entrance channels were generally well predicted by the Hauser-Feshbach calculations. The agreement between the calculations and experimental cross sections implies that compound nuclear formation dominates these reactions. Poor agreement, however, was obtained between the experimental and calculated ^{4}He and ^{8}Be cross sections for the $^{7}Li+ {}^{16}O$ entrance channel. All cross sections for this case were substantially underpredicted. Reasonable variations of the level density parameters (10%) did not reproduce the $^{7}Li+ {}^{16}O$ experimental data. The use of other $^{7}Li+ {}^{16}O$ optical model parameter sets produced little change in the predicted ^{4}He and ^{8}Be cross sections for the $^{7}Li+ {}^{16}O$ en-

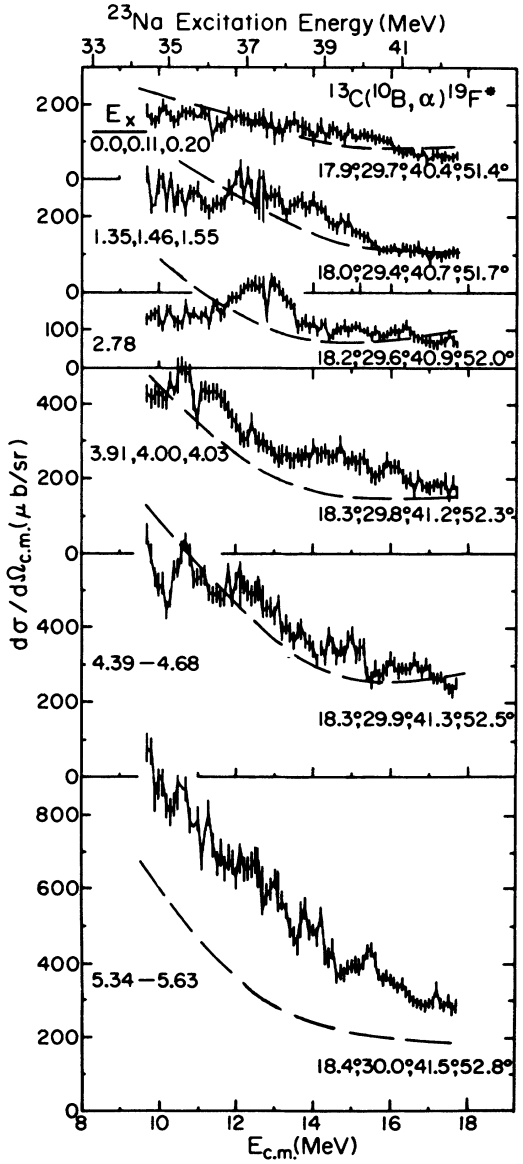

FIG. 2. Excitation functions for the $^{10}B+ {}^{13}C$ reaction leading to the α-particle exit channel. The energies of the residual ^{19}F states are in MeV. See Fig. 1 for a further explanation of the figure.

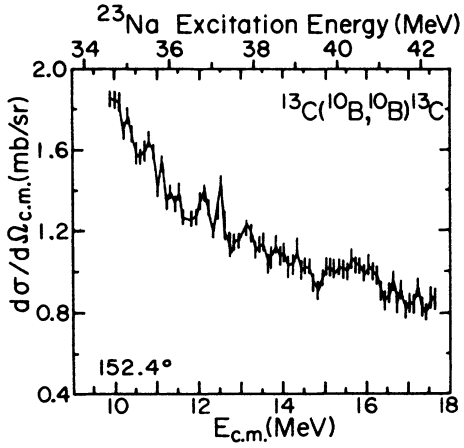

FIG. 3. Elastic scattering excitation functions for the $^{10}B+ {}^{13}C$ entrance channel.

trance channel. As mentioned previously, the calculated cross sections do depend upon the critical angular momenta. However, as the critical angular momenta for all three entrance channels were obtained in a consistent manner, no justification can be made for arbitrarily altering the critical angular momenta for one of the three sets. The $^{7}Li+ {}^{16}O$ results, therefore, suggest the presence of some other reaction process, such as direct transfer, in that entrance channel.

B. Search for nonstatistical structure

The problem related to the identification of nonstatistical structure in a fluctuating excitation function has been discussed extensively in the literature. In a system like $^{12}C+ {}^{16}O$, where the resonance structure is quite strong, the correlations over angle and among different exit channels can readily be seen by eye.[6] However, the structures seen in systems having nonzero channel spins are expected to be smaller simply due to the statistical spin factor.[5] Even so, if a visually weak structure is correlated over a large angular range and among different exit channels, then it may in fact be highly nonstatistical. To assist in the identification of nonstatistical structure in the present experiment we have used the deviation function and the distribution of maxima test.[14] Each approach has its own strengths and weaknesses. A brief discussion of these two types of analyses is needed.

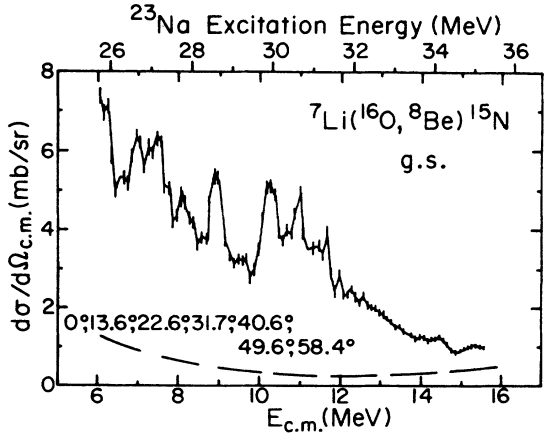

FIG. 4. Excitation functions for the $^{7}Li+ {}^{16}O$ reaction leading to the ^{8}Be exit channel. The energies of the residual ^{15}N states are given in MeV. See Fig. 1 for a further explanation of the figure.

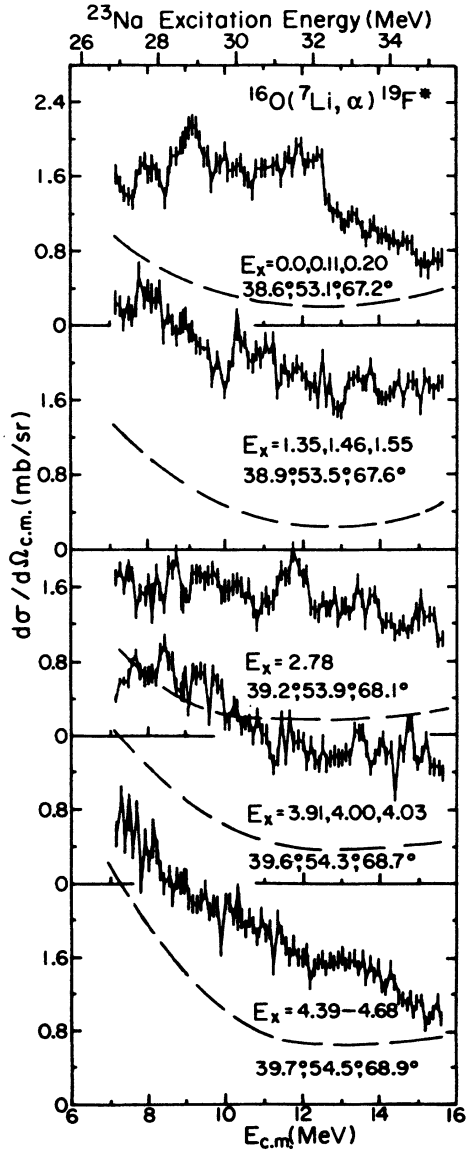

FIG. 5. Excitation functions for the $^{7}Li+ {}^{16}O$ reaction leading to the ^{4}He exit channel. The energies of the residual ^{19}F states are in MeV. See Fig. 1 for a further explanation of the figure.

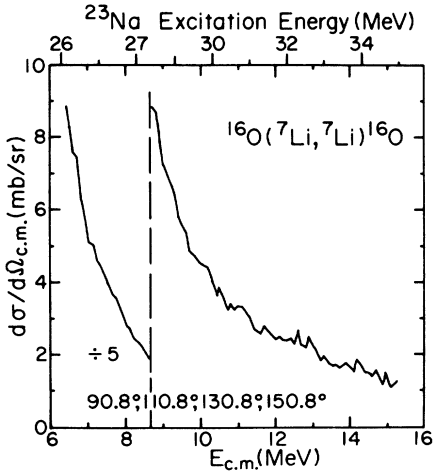

FIG. 6. Elastic scattering excitation functions for the ^{7}Li+ ^{16}O entrance channel. The angles listed are in the center of mass.

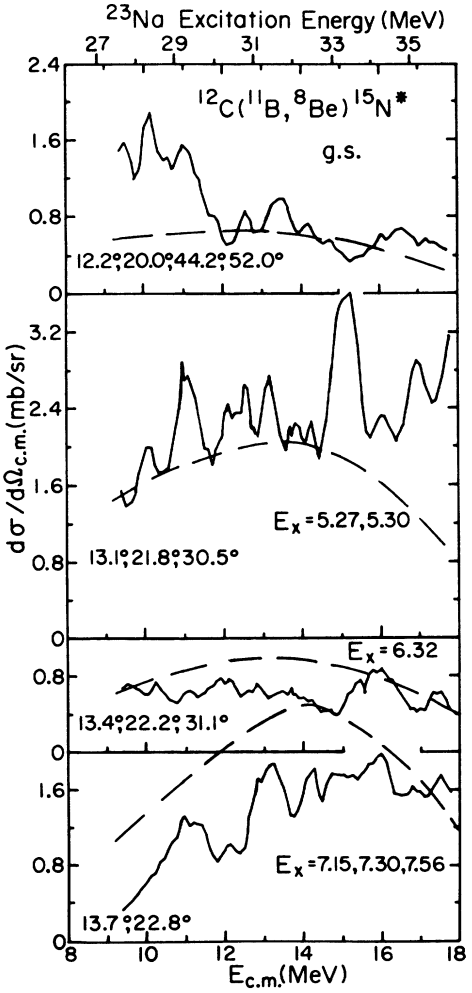

FIG. 7. Excitation functions for the ^{11}B+ ^{12}C reaction leading to the ^{8}Be exit channel. The energies of the residual ^{15}N states are given in MeV. The uncertainties in this set of ^{8}Be data are approximately the size of each data point. See Fig. 1 for a further explanation of the figure.

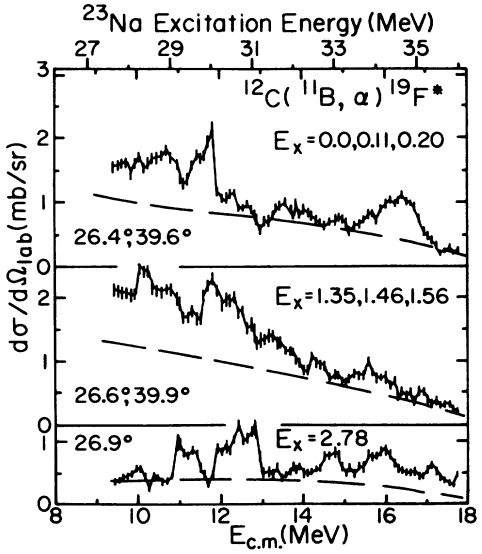

FIG. 8. Excitation functions for the ^{11}B+ ^{12}C reaction leading to the ^{4}He exit channel. The energies of the residual ^{19}F states are in MeV. See Fig. 1 for a further explanation of the figure.

The deviation function is defined as

$$D(E)=(1/N)\sum_{i=1}^{N}\left[\frac{\sigma_i(E)}{\langle\sigma_i(E)\rangle}-1\right],$$

where N is the number of excitation functions and $\langle\sigma_i(E)\rangle$ is a moving average for excitation function i. Care must be exercised when interpreting the results obtained from a deviation function analysis. A maximum

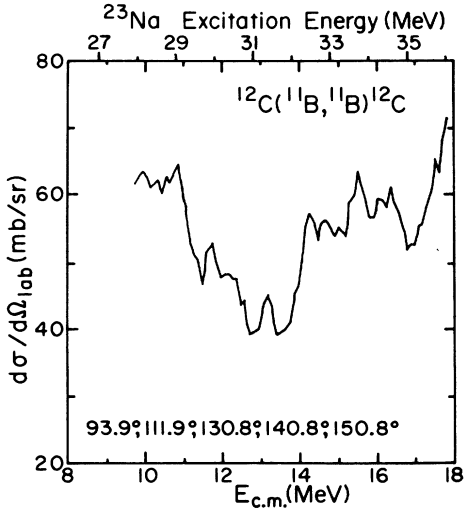

FIG. 9. Elastic scattering excitation function for the ^{11}B+ ^{12}C entrance channel. The angles listed are in the center of mass.

TABLE III. Level density parameters used in the Hauser-Feshbach analysis.

Channel[a]	E_0 (MeV)	T (MeV)	a (MeV^{-1})	E_x (MeV)
n+ ^{22}Na	−2.52	2.71	2.90	10.35
P+ ^{20}Ne	1.02	2.43	3.64	16.75
d+ ^{21}Ne	−0.48	2.33	3.53	12.39
t+ ^{20}Ne	1.88	2.88	2.76	16.40
^{4}He+ ^{19}F	−2.08	2.96	2.94	16.42
^{5}He+ ^{18}F	−2.61	2.76	3.05	10.31
^{6}Li+ ^{17}O	−1.29	3.27	2.66	15.53
^{7}Li+ ^{16}O	1.10	2.94	3.00	20.10
^{8}Be+ ^{15}N	2.65	4.71	1.24	9.75
^{10}B+ ^{13}C	−2.42	5.50	1.47	21.25
^{11}B+ ^{12}C	0.56	6.93	1.05	22.73

[a]Parameters are for heavy particle only.

or a minimum will be produced in the above function if a maximum or a minimum occurs at the same energy in several of the excitation functions. However, a maximum or minimum can also be produced in the above function if even one excitation function has a very strong maximum or minimum. The primary weakness of the deviation function as a test for correlated structure is that weak but well correlated peaks may appear less prominently than a single strong fluctuation in one excitation function.

While the deviation function is useful in attempting to locate correlated structure, there is, unfortunately, no direct relationship between $D(E)$ and correlations between exit channels. The distribution of maxima test, on the other hand, can be used to judge whether or not a structure is consistent with the statistical model. This test consists of counting the number of maxima which occurs at a particular energy interval in a set of excitation functions. If a resonance is present, it will result in an anomalously large number of maxima at a given excitation energy. In this analysis, a comparison is made between the statistically predicted number of energy intervals, $N_s(\Delta E,M)$, of width ΔE, for which cross section maxima are to appear in M reaction channels, with the actual number observed, $N_0(\Delta E,M)$.

The probability of observing M maxima within an energy interval ΔE in m excitation functions is given by the binomial distribution

$$P(M)=\frac{m!p^M(1-p)^{m-M}}{M!(m-M)!} ,$$

where p is the probability of finding a maximum in a randomly placed energy interval ΔE in any of the m excitation functions. In practice, p is approximated by letting $p=n_+/n$, where n_+ is the number of intervals exhibiting maxima and n is the total number of intervals in the m excitation functions. The uncertainty in $P(M)$ is evaluated by using the statistical error in the value of p,

$$\Delta p=[p(1-p)/n]^{1/2} .$$

Finally, the number of statistically predicted intervals exhibiting maxima in M channels is given by

$$N_s(\Delta E,M)=(n/m)P(M) .$$

In the experimental excitation functions, a maximum was taken to be any point whose cross section was greater than that of its nearest neighbors, and such that the cross sections decreased sufficiently at higher and lower energies, that the error bars do not overlap with the error at the maximum cross section. Sampling energy intervals ΔE of 200 keV (twice the data point spacing) were used in the analysis. Smaller sampling intervals would be expected to reduce the number of observed correlations because the energy of cross section maxima may be expected to shift by half a coherence width. When larger values of ΔE are used, the number of observed correlations is again reduced as some of the energy intervals contain more than one maximum. Finally, as it is difficult to identify precisely the energy of structure in elastic scattering data

TABLE IV. Optical model parameters used in the Hauser-Feshbach analysis.

Channel	V[a] (MeV)	r_r[b] (fm)	a_r (fm)	W[a] (MeV)	r_i[b] (fm)	a_i (fm)	Type
n+ ^{22}Na	47.01−0.27E	0.94	0.66	9.53−0.053E	0.94	0.48	Surface
p+ ^{20}Ne	52.70−0.55E	0.94	0.65	13.50	0.94	0.47	Surface
d+ ^{21}Ne	89.30−0.22E	0.78	0.81	14.40+0.24E	0.91	0.68	Surface
t+ ^{20}Ne	153.5	0.74	0.69	30.50	0.94	0.89	Surface
^{4}He+ ^{19}F	130.0	0.83	0.63	44.90	0.83	0.35	Volume
^{5}He+ ^{18}F	7.50+0.4E	1.35	0.45	0.4+0.13E	1.35	0.45	Volume
^{6}Li+ ^{17}O	7.50+0.4E	1.35	0.45	0.4+0.13E	1.35	0.45	Volume
^{7}Li+ ^{16}O	95.0	1.73	0.78	7.80	2.39	0.89	Volume
^{8}Be+ ^{15}N	26.70	1.25	0.95	25.0	1.25	0.95	Volume
^{10}B+ ^{13}C	66.85	1.09	0.61	10.0	1.20	0.70	Volume
^{11}B+ ^{12}C	60.5	1.09	0.61	36.04	1.18	0.49	Volume

[a]All energy dependent potentials have energy dependences which are computed in the center of mass, i.e., $E=E_{\text{c.m.}}$.
[b]$R=r_{r,i}(A_t^{1/3}+A_p^{1/3})$.

TABLE V. Summary of structure correlation for the $^{11}B+^{12}C$, $^{7}Li+^{16}O$, and $^{10}B+^{13}C$ entrance channels. All center-of-mass and excitation energies are in MeV. The presence of an × signifies that a peak was observed while a * indicates that no peak was observed. A blank has been used when no excitation function for the particular excited state was measured.

$E_{c.m.}$	^{19}F						^{15}N				
(MeV)	g.s.	1.5	2.8	4.0	4.7	5.5	g.s.	5.3	6.3	7.3	$P(M)$
$^{11}B+^{12}C$											
10.95	*	*	×				×	×	×	×	0.008
16.0	*	*	×				×	×	×	×	0.008
$^{7}Li+^{16}O$											
none											
$^{10}B+^{13}C$											
10.5	×	×	*	×	*	×	×	×	*	×	0.005

due to the interference effects, none of the elastic scattering excitation functions were included in the probability analysis.

The results of the probability analysis are presented in Table V for the ^{4}He and ^{8}Be exit channels for each of the three entrance channels. Only those structures which produced a low probability of being statistical, arbitrarily chosen to be $<1\%$, have been listed. A probability of less than 1% means that for a given set of excitation functions, less than 1 such event should be observed for every 100 energy intervals.

For the $^{11}B+^{12}C$ entrance channel, the 1% probability criterion is met at only two energies, 10.95 and 16.0 MeV. As can be seen in Fig. 10, the 10.95 and 16.0 MeV structures show positive values in the $^{11}B+^{12}C$ deviation function $D(E)$. Structure is also clearly present at 16 MeV in the angle-summed $^{11}B+^{12}C$ elastic scattering data in Fig. 9. The additional structures listed in Ref. 5 at $E_{c.m.}=10.1$, 11.7, 12.5, 13.2, 14.2, 14.8, and 15.3 MeV did not give rise to probabilities of less than 1%.

For the $^{7}Li+^{16}O$ entrance channel, none of the structures had probabilities $<1\%$. The deviation function for this entrance channel is shown in Fig. 11.

The $^{10}B+^{13}C$ entrance channel exhibited one energy at which the structure was correlated over a sufficient number of exit channels to produce a probability $<1\%$. This structure occurs at an energy of 10.5 MeV. As seen in Fig. 12, a positive value for $D(E)$ is found at this energy.

Of course, some low probability events should be expected even for a sample which is purely statistical. A comparison of the distribution of maxima for a statistically predicted number of energy intervals, $N_s(\Delta E,M)$, with the number actually observed in each of the three entrance channels is presented in Fig. 13. For both the $^{7}Li+^{16}O$ and $^{10}B+^{13}C$ entrance channels, there is excellent agreement between the statistically predicted distribution and the number observed experimentally. This suggests that all of the structures, even those with small probabilities, may have a statistical origin. For the $^{11}B+^{12}C$ entrance channel, the number of energy inter-

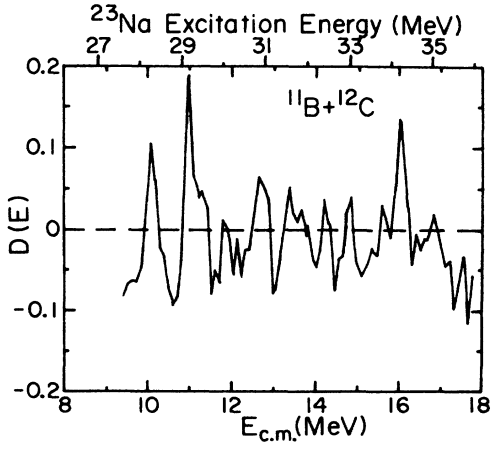

FIG. 10. Results of the deviation function analysis for the $^{11}B+^{12}C$ entrance channel. All of the final states shown in Figs. 7 and 8 were included in the analysis.

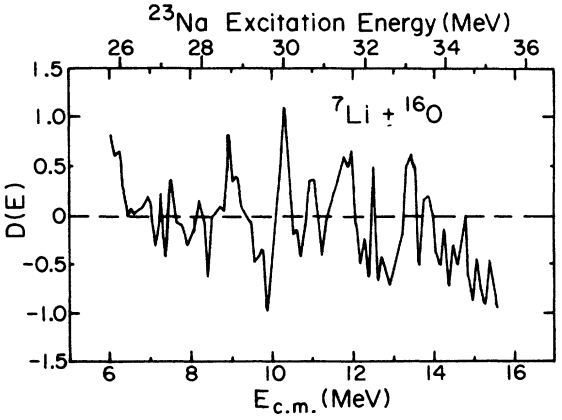

FIG. 11. Results of the deviation function analysis for the $^{7}Li+^{16}O$ entrance channel. All of the final states shown in Figs. 4 and 5 were included in the analysis.

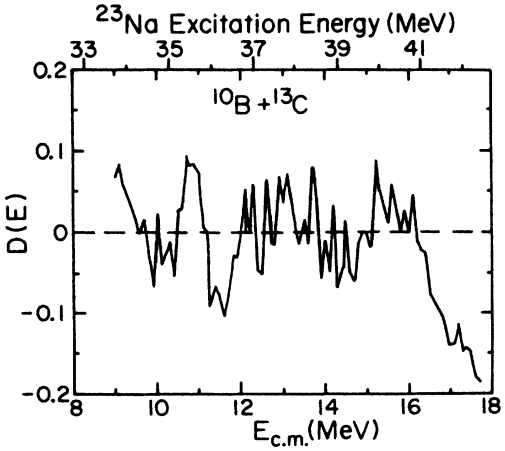

FIG. 12. Results of the deviation function analysis for the ^{10}B+ ^{13}C entrance channel. All of the final states shown in Figs. 1 and 2 were included in the analysis.

vals which show correlations among four and five exit channels ($M=4$ and 5 for the ^{11}B+ ^{12}C entrance channel in Fig. 13) is larger than would be expected for a purely statistical distribution. Such a result could indicate the presence of resonances. The difference between the experimental and predicted results is not so overwhelming, however, that one can unambiguously state that resonances exist in the ^{11}B+ ^{12}C system.

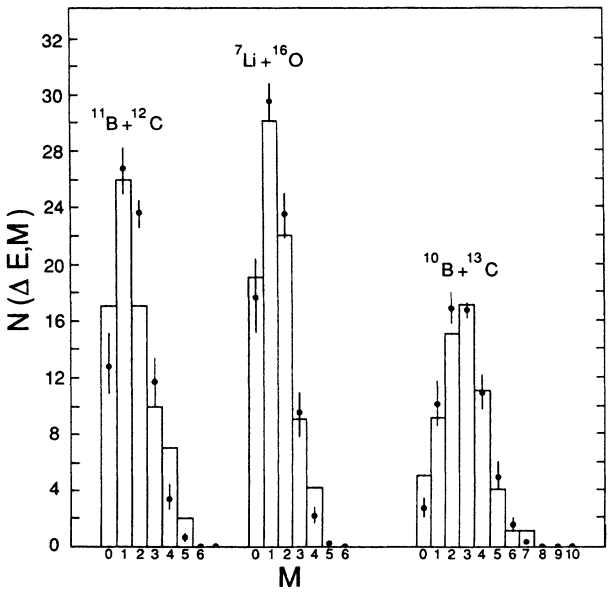

FIG. 13. Number of energy intervals, $N(\Delta E,M)$, of width ΔE which have cross section maxima in M exit channels for the ^{11}B+ ^{12}C, ^{7}Li+ ^{16}O, and ^{10}B+ ^{13}C entrance channels. The histograms represent the experimentally observed number N_0, while the points are calculations based on a random occurrence of maxima, N_s, with associated statistical errors.

IV. DISCUSSION

A. Entrance channel versus compound nuclear properties and resonance formation

Early experimental investigations like those of Hanson *et al.*[15] and theoretical studies like that of Pocanic and Cindro[16] focused primarily on the level density in the compound nucleus in their attempts to explain heavy-ion resonance formation. For heavy-ion resonances to be isolated states in the compound nucleus, it was believed that the entrance channel must form the compound system in a region of low compound-nuclear level density. Entrance channels forming compound nuclei with high level densities, examples of which are ^{26}Al, ^{27}Al, and ^{30}Si, were not expected to exhibit resonances. Several studies now report that resonances are formed in these compound nuclei using the ^{12}C+ ^{14}N (Refs. 14 and 17), ^{12}C+ ^{15}N (Ref. 18), and ^{12}C+ ^{18}O (Ref. 19) entrance channels, respectively.

More recently, studies by Thornton *et al.*[2] and Parks *et al.*[3] have suggested that the entrance channel binding energy E_B and, to a lesser extent, the effective entrance channel moment of inertia, are also important. Which compound-nuclear states will be populated at a particular compound nucleus excitation energy must depend upon the angular momentum available to the system. If an entrance channel's binding energy is small, then a larger center-of-mass energy $E_{c.m.}$ will be required to reach a particular compound nucleus excitation energy E_x^* (i.e., $E_x^*=E_{c.m.}+E_B$). An increase in the center-of-mass energy, of course, increases the angular momentum available to the compound nucleus. This increases the likelihood that a semi-isolated, high-spin state will be formed. The population of such a state could produce structure like that seen in heavy-ion excitation functions.

For the ^{23}Na compound nucleus, the binding energies for the ^{11}B+ ^{12}C, ^{7}Li+ ^{16}O, and ^{10}B+ ^{13}C entrance channels are 18.2, 19.7, and 24.7 MeV, respectively. According to the model proposed by Thornton *et al.*[2], the ^{11}B+ ^{12}C entrance channel should be the most likely to exhibit resonances while the ^{10}B+ ^{13}C should be least likely.

Our results support this qualitative picture. Of the three entrance channels which form the ^{23}Na compound nucleus, the only one which exhibits any deviation from a purely statistical interpretation is the ^{11}B+ ^{12}C, the system with the lowest binding energy.

B. Do different entrance channels form the same heavy-ion resonances?

In the earlier work of Parks *et al.*,[3] no evidence was found that different entrance channels formed the same nonstatistical structures in any of the ^{26}Al, ^{29}Si, or ^{30}Si compound nuclei. A similar search has been carried out in our study of ^{23}Na.

In the present investigation, both the ^{11}B+ ^{12}C and ^{7}Li+ ^{16}O entrance channels form the ^{23}Na compound nucleus over an excitation energy range from 28.2 to 35.3 MeV. Further, at a ^{23}Na excitation energy of 30 MeV, for example, the ^{11}B+ ^{12}C and ^{7}Li+ ^{16}O entrance chan-

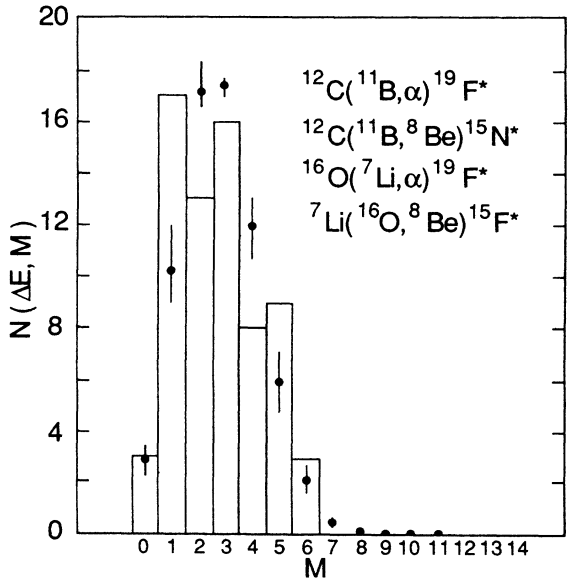

FIG. 14. Number of energy intervals, $N(\Delta E,M)$, of width ΔE which have cross section maxima in M exit channels. All ^{4}He and ^{8}Be excitation functions from both the ^{7}Li+ ^{16}O and ^{11}B+ ^{12}C entrance channels have been included in the analysis. A ^{23}Na excitation energy range from 28.2 to 35.2 MeV was covered.

nels have grazing angular momenta of $9.8\hbar$ and $8.5\hbar$, respectively.[7] When coupled to their entrance channel spins, angular momentum ranges of $8.3\hbar < J < 11.3\hbar$ and $7\hbar < J < 10\hbar$ are found for the ^{11}B+ ^{12}C and ^{7}Li+ ^{16}O systems, respectively. With this overlap in angular momentum, some formation of common resonances might be possible.

The results of our distribution of maxima analysis which employed all of the ^{4}He and ^{8}Be exit channels for both the ^{7}Li+ ^{16}O and ^{11}B+ ^{12}C entrance channels are presented in Fig. 14. As can be seen in this figure, there is little evidence that the two entrance channels form the same heavy-ion resonances. The experimental distribution of maxima are adequately reproduced by a purely statistical model.

V. CONCLUSIONS

A search has been conducted for nonstatistical structure in three non-α-conjugate entrance channels, ^{10}B+ ^{13}C, ^{7}Li+ ^{16}O, and ^{11}B+ ^{12}C, which lead to the ^{23}Na compound nucleus. The exit channels studied for all three entrance channels were the ^{4}He, ^{8}Be, and the elastic. Structures which were correlated over a large number of exit channels and, consequently, exhibited low probabilities of being statistical in origin, were observed at energies of 10.95 and 16 MeV in the ^{11}B+ ^{12}C entrance channel and at an energy of 10.5 MeV in the ^{10}B+ ^{13}C excitation functions. No strongly correlated structures were found in the ^{7}Li+ ^{16}O data.

The distribution of maxima test for the ^{10}B+ ^{13}C and the ^{7}Li+ ^{16}O entrance channels leads us to the conclusion that these reactions are dominated by statistical processes and that no strong evidence of resonances is present. In the case of the ^{11}B+ ^{12}C entrance channel, poorer agreement between the observed and predicted statistical distribution of maxima was obtained. Such a result could indicate the presence of resonances in this entrance channel.

If resonances are indeed formed by the ^{11}B+ ^{12}C entrance channel and not by the ^{7}Li+ ^{16}O and ^{10}B+ ^{13}C channels as our analysis implies, the model proposed by Thornton *et al.*[2] which suggests that resonance formation depends upon entrance channel binding energy and moment of inertia accurately describes our experimental results.

Finally, in both the present study and the earlier investigation by Parks *et al.*,[3] no two entrance channels which form the same compound nucleus populate the same nonstatistical structure. This, despite the fact that the entrance channels which form the same compound nucleus, do so with similar angular momenta. The implication of this result is that the nuclear states which are being populated are strongly dependent upon the entrance channel configuration.

ACKNOWLEDGMENTS

The assistance of Melissa Syter in carrying out the statistical analysis was greatly appreciated. This work has been supported in part by the U.S. Department of Energy under Contract No. DE-AS05-80ER10714 and by the National Science Foundation under Grant No. PHY-8303455.

*Present address: Physics Department, University of South Florida, Tampa, FL 33620.

[1] D. A. Bromley, J. A. Kuehner, and E. Almquist, Phys. Rev. Lett. **4**, 365 (1960); D. A. Bromley, J. A. Kuehner, and E. Almquist, Phys. Rev. **123**, 878 (1961); M. Feil, W. Von Oertzen, H. G. Bohlen, A. Gamp, and R. L. Walter, Z. Phys. **260**, 271 (1973); D. A. Bromley, in *Proceedings of the Second International Conference on Clustering Phenomena in Nuclei, College Park, Maryland, 1975,* edited by D. A. Goldberg, J. B. Marion, and S. J. Wallace (National Technical Information Service, Springfield, Virgina, 1975), and references therein; J. Gomez del Campo. J. L. C. Ford, Jr., R. L. Robinson, M. E. Ortiz, A. Dacal, and E. Andrade, Phys. Lett. **69B**, 415 (1977); J. F. Mateja, A. D. Frawley, A. Roy, J. Hurd, and N. R. Fletcher, Phys. Rev. C **18**, 2622 (1978); T. M. Cormier, C. M. Jachcinski, G. M. Berkowitz, P. Braun-Munzinger, P. M. Cormier, M. Gai, J. W. Harris, J. Barrette, and H. E. Wegner, Phys. Rev. Lett. **40**, 924 (1978); R. E. Malmin, J. W. Harris, and P. Paul, Phys. Rev. C **18**, 163 (1978); P. Taras, in *Clustering Aspects of Nuclear Structure and Nuclear Reactions,* Proceedings of the Third International Conference on Clustering Aspects of Nuclear Structure and Nuclear Reactions, AIP Conf. Proc. No. 47, edited by W. T. H. Van Oers, J. P. Svenne, J. S. C. McKee, and W. R. Falk (AIP, New York,

1978), p. 234, and references therein.
[2]S. T. Thornton, L. C. Dennis, and K. R. Cordell, Phys. Lett. **91B**, 196 (1980).
[3]R. L. Parks, S. T. Thornton, K. R. Cordell, and C. A. Wiedner, Phys. Rev. C **25**, 313 (1982).
[4]A. D. Frawley, J. F. Mateja, A. Roy, and N. R. Fletcher, Phys. Rev. Lett. **41**, 846 (1978).
[5]A. D. Frawley, J. F. Mateja, A. Roy, and N. R. Flecher, Phys. Rev. C **19**, 2215 (1979).
[6]J. R. Hurd, N. R. Fletcher, A. D. Frawley, and J. F. Mateja, Phys. Rev. C **22**, 528 (1980).
[7]J. F. Mateja, A. D. Frawley, L. C. Dennis, K. Abdo, and K. W. Kemper, Phys. Rev. C **25**, 2963 (1982); J. F. Mateja, J. Garman, D. E. Fields, R. L. Kozub, A. D. Frawley, and L. C. Dennis, *ibid.* **30**, 134 (1984).
[8]D. L. Gay, L. C. Dennis, and N. R. Fletcher, Phys. Rev. C **34**, 2144 (1986).
[9]G. R. Morgan and N. R. Fletcher, Phys. Rev. C **16**, 167 (1977).
[10]H. G. Bingham, A. P. Zandler, K. W. Kemper, and N. R. Fletcher, Nucl. Phys. **A173**, 265 (1971).
[11]S. K. Penny, private communication.
[12]L. C. Dennis, A. Roy, A. D. Frawley, and K. W. Kemper, Nucl. Phys. **A359**, 455 (1981).
[13]H. V. Klapdor, H. Reiss, and G. Rosner, Nucl. Phys. **A262**, 157 (1976).
[14]L. C. Dennis, S. T. Thornton, and K. R. Cordell, Phys. Rev. C **19**, 777 (1979).
[15]D. L. Hanson, R. G. Stokstad, K. A. Erb, C. Olmer, M. W. Sachs, and D. A. Bromley, Phys. Rev. C **9**, 1760 (1974).
[16]D. Pocanic and N. Cindro, J. Phys. G **5**, L25 (1979).
[17]K. R. Cordell, C. A. Wiedner, and S. T. Thornton, Phys. Rev. C **23**, 2035 (1981).
[18]J. Gomez del Campo, J. L. C. Ford, Jr., R. L. Robinson, M. E. Ortiz, A. Dacal, and E. Andrade, Phys. Lett. **69B**, 415 (1977).
[19]M. P. Webb, R. Vandenbosch, K. A. Eberhard, K. G. Bernhardt, and M. S. Zisman, Phys. Rev. Lett. **36**, 779 (1976).